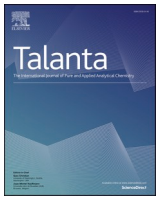
Talanta 266 (2024) 125039



Contents lists available at ScienceDirect

Talanta

journal homepage: www.elsevier.com/locate/talanta





Highly-efficient selection of aptamers for detecting various HPV subtypes in clinical samples

Guotai Yang [a], Wei Li [a], Shun Zhang [a], Bei Hu [a], Zhen Huang [a,b,c,*]

[a] Key Laboratory of Bio-Resource and Eco-environment of Ministry of Education, College of Life Sciences, Sichuan University, Chengdu, Sichuan, 610064, PR China
[b] State Key Laboratory of Southwestern Chinese Medicine Resources, Chengdu University of Traditional Chinese Medicine, Chengdu, Sichuan, 610000, PR China
[c] SeNA Research Institute and Szostak-CDHT Large Nucleic Acids Institute, Chengdu, Sichuan, 610095, PR China

ARTICLE INFO

Handling Editor: J.-M. Kauffmann

Keywords:
In vitro selection
SELEX
Aptamer
HPV detection
Clinical sample diagnosis

ABSTRACT

Nucleic acid aptamers are of great potentials in diagnostic and therapeutic applications because of their unique molecular recognition capabilities. However, satisfactory aptamers with high affinity and specificity are still in short supply. Herein, we have developed new selection methods allowing the free interactions between the targets and potential aptamers in solution. In our selection system, the protein targets (biotinylated randomly or site-specifically) were first incubated with the random DNA library, followed by the pull-down with the streptavidin magnetic beads or biolayer-interferometry (BLI) sensors. By comparing the two biotinylation strategies (random or site-specific) and two states of the targets (free or immobilized), we have found that the combination of the site-specific biotinylation and free-target strategies was most successful. Based on these highly-efficient selection strategies, HPV L1 aptamers were obtained. By designing the sandwich aptasensor assisted with RCA and CRISPR/Cas12a, we have diagnosed various HPV subtypes in clinical samples, such as easily-collected urine samples. In summary, our new strategy can allow efficient selection of aptamers with high affinity and specificity for clinical applications.

1. Introduction

The first aptamers were found via molecular selection [1,2], and they are DNA or RNA oligonucleotides with defined 3D structures [3]. Generally, aptamers are selected via the *in vitro* selection [1] or Systematic Evolution of Ligands by Exponential enrichment (SELEX) [2]. The selected aptamers have demonstrated great potentials in exploring the innovative therapeutics, diagnostics, drug delivery, and bio-sensing [4–7]. Aptamers can specifically recognize the targets (including proteins, nucleotides, metal ions, small molecules, and cells) with high affinity and specificity [8–13]. Over the past three decades, many strategies, such as the selections based on beads [14–16], microfluidics [17], target-capture [18], capillary electrophoresis [19,20], in silico selection [21] and cell SELEX [12], have been developed. However, efficiencies of most strategies are low, thereby the satisfactory aptamers with high affinity and specificity are in short supply for clinical applications. The identified aptamers usually suffer in the poor chemical and biological stability, structural flexibility, and nonspecific interactions, which limit their applications. The poor selection efficiency is attributed to the inefficient enrichment, monotonous selection environment, mild selection conditions, complex selection operation, equipment dependency, and library limitation [22–26]. In order to identify high-quality aptamers, more efficient selection strategies need to be developed.

The free- or immobilized-binding mode between targets and potential aptamers, which directly affects their interactions and outcomes, is one of the critical factors for the selection efficiency. Unfortunately, most strategies don't pay attention to the binding modes. Immobilization of the targets or aptamer libraries can jeopardize the selection efficiency. As we know, the traditional SELEX methods depend on target immobilization on the certain surfaces and solid supports [e.g., magnetic beads [16], microfluidic chips [27], surface plasmon resonance (SPR) sensors [28] and biolayer-interferometry (BLI) sensors [29]], thereby limiting the target freedom and binding areas, and increasing the target polymorphism. Further, some efforts to immobilize libraries have been attempted, which keeps the targets free to ensure their integrity and thorough interactions with the libraries, such as aptamer particles (AP)-based selection [24,30] and capture SELEX [18]. In AP-based SELEX, multiple copies of an identical sequence were displayed on the surface of one particle, forming the AP library. In capture SELEX, the

* Corresponding author. 17, Section 3, Renmin South Road, Chengdu, 610064, PR China.
E-mail address: Huang@SeNAresearch.org (Z. Huang).

https://doi.org/10.1016/j.talanta.2023.125039
Received 10 June 2023; Received in revised form 31 July 2023; Accepted 4 August 2023
Available online 5 August 2023
0039-9140/© 2023 Published by Elsevier B.V.

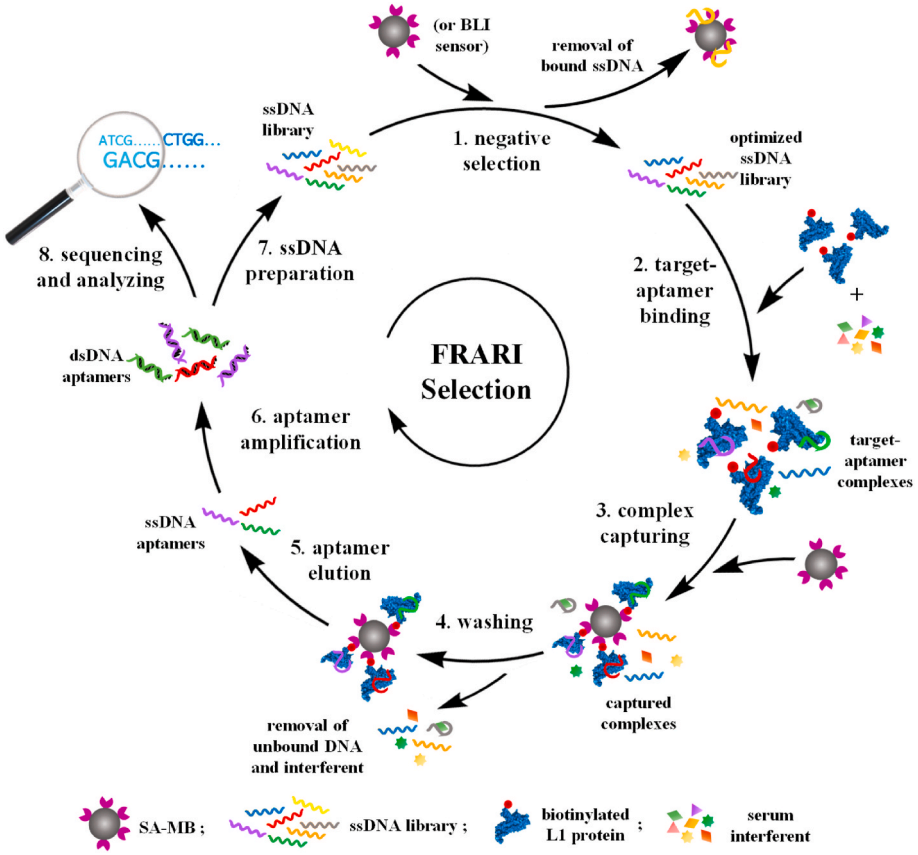


Fig. 1. Overview of the FRARI selection.

aptamer library was anchored to solid supports by duplex formation, and the free targets, binding to the library and disrupting the duplex, release the aptamer molecules from the supports. Inappropriate immobilizations increase the non-specific interaction, enrich low-affinity sequences, and decrease the selection efficiency of high-affinity aptamers [31]. Furthermore, the strategies with both free targets and libraries have been explored, such as capillary electrophoresis (CE)-SELEX [19,20,32] and magnetic cross-linking precipitation (MCP)-SELEX [22]. The CE method allows the target interaction with libraries in a free-binding mode, and the formed target-aptamer complexes are separated by CE. In MCP-SELEX, the formed target-aptamer complexes were separated based on the cross-linking reaction of the target amino groups with the carboxylic acid groups on magnetic particles. Although more efforts have focused on both free targets and library strategies in recent years [33–35], these strategies are not compatible with the complex environments (such as serum).

To face the selection challenges, we have developed a new method, namely free aptamer-ligand interaction (FRARI) selection (Fig. 1). HPV L1 protein, as the major capsid proteins, is a critical target for HPV detection. In our study, L1 protein was chosen as a testing target for selection, and the selection has taken advantage of the free interaction between the biotinylated targets and potential aptamers, followed by the pull-down with the streptavidin-magnetic beads (SA-MBs) or BLI SA-sensors; the isolated DNAs are amplified and used for the next round of selection. The biotinylated targets are prepared by random cross-linking [36] or the site-specific modification on the avi tag by biotin protein ligase (BPL) [37]. By comparing these two biotinylation strategies and two binding modes, we have found that the combination of the site-specific biotinylation and free-target strategies are most efficient. By conducting the selection in the complex environments (such as serum), our strategy has offered the highly-efficient aptamers for diagnosing simultaneously several HPV virus subtypes in clinical samples via its L1 protein detection, as their L1 proteins have the high sequence homology and similar structures. Using the selected aptamers and their sandwich structures, we have constructed a FRARI detection (FRARI-selected aptamer-sandwich detection assisted with RCA and CRISPR/Cas12a) method for HPV detection. Many HPV subtypes in clinical samples (such as urine samples collected easily and patient-friendly) have been successfully detected, indicating the effectiveness and practicability of FRARI selection in identifying aptamers for clinical applications.

2. Experimental section

Parts of the experimental sections were described in the supplementary material.

2.1. Target-immobilized SELEX for HPV L1

HPV L1 biotinylated with random or site-specific strategy was immobilized on SA-MBs. Briefly, the biotinylated L1 was immobilized on SA-MBs using the mole ratio (L1:SA = 10:1), and the mixture was incubated at room temperature for 2 h, followed by the blocking for 1 h with 1% (w/v) BSA solution.

Initial library (10 μL, 100 μM; Table S1) or enriched ssDNA was diluted in PBS (490 μL) and incubated at 95 °C for 10 min, followed by quick placement on ice for 10 min, and subsequently placed at room temperature for 10 min. The L1-modified MBs (25 μg) were subsequently added into the library, followed by incubating the mixture at room temperature for 1 h. Then the formed complexes were collected by an external magnetic field, washed for 4 times with PBS, and resuspended with PBS (100 μL). Subsequently, proteinase K (1.8 μL, 20 mg/mL) was added, and the mixture was incubated in 52 °C for 2 h. After removal of the MBs with a magnetic field, the supernatant was incubated in 95 °C for 20 min to release DNA as templates for PCR. Then, the PCR

amplification was performed in the reaction (50 μL) with DNA templates (5 μL), two primers (each 5 μL, 10 μM), 2 × Taq Mix (25 μL) and ddH_2O (10 μL). The PCR conditions were 95 °C for 10 min, followed by 20 cycles of 94 °C for 30 s, 61 °C for 30 s, and 72 °C for 30 s. The PCR products were purified using the TaKaRa MiniBest DNA Fragment Purification Kit (TaKaRa Biotech Co. Ltd., Dalian, China) using the manufacturer's protocol. λ exonuclease was applied to digest the phosphorylated strand to generate the ssDNA. The ethanol precipitation was performed, and the ssDNA was collected. The purified ssDNA was used for the next round of the target-immobilized SELEX. In performing the later selections, we gradually strengthened the conditions: 1) reducing the ssDNA amount (to 0.2 nmol after round 4), 2) applying the negative selection using the SA-MBs without immobilized L1 (after round 7), 3) reducing the incubation time between the protein and the ssDNA (20 min after round 8), and 4) adding serum (20% at the final concentration after round 10) to increase environmental complexity. To study the effectiveness of the selection, the PCR-amplification products from round 3, 6, 9 and 15 were sequenced at Sangon Biotech Co. Ltd. (Shanghai, China), and the sequencing results were analyzed by FASTAptamer.

2.2. SA-MB-based FRARI selection for HPV L1

HPV L1 biotinylated with random or site-specific strategy was applied in SA-MB-based FRARI selection. Initial library (10 μL, 100 μM, Table S1) or enriched ssDNA was prepared as described above. Randomly-biotinylated L1 (0.50 μg) or site-specifically-biotinylated L1 (0.30 μg) was added into the library or ssDNA, followed by incubating the mixture at room temperature for 1 h. Subsequently, SA-MBs were added into the mixture, followed by incubating at room temperature. Then, the MB-captured complexes were collected by an external magnetic field, washed for 4 times with PBS, and resuspended with PBS (100 μL). The other steps to obtain ssDNA for next round selection were as same as the described above. In performing the later selections, we gradually strengthened the conditions: 1) reducing the ssDNA amount (to 0.2 nmol after round 3), 2) applying the negative selection using the SA-MBs without immobilized L1 (after round 4), 3) reducing the incubation time between the protein and the ssDNA (20 min after round 4), and 4) adding serum (20% at the final concentration after round 6) to increase environmental complexity. To study the effectiveness of the selection, the PCR-amplification products from round 3, 6 and 9 were sequenced at Sangon Biotech Co. Ltd. (Shanghai, China), and the sequencing results were analyzed by FASTAptamer.

2.3. BLI-based FRARI selection for HPV L1

Initial library (10 μL, 100 μM, Table S1) or enriched ssDNA was diluted in PBS (190 μL) and prepared as described above. Randomly-biotinylated L1 (0.625 μg) or site-specifically-biotinylated L1 (0.3 μg) was added into the library or ssDNA, followed by incubating the mixture at room temperature for 1 h. The BLI SA-sensor was used to capture the formed complexes by incubating the sensor with the mixture for 50 min. After washing twice with PBS (once for 600 s and once for 120 s), the captured complexes were digested in PBS (100 μL) with proteinase K (1.8 μL, 20 mg/mL) in 52 °C for 2 h. The other steps to obtain ssDNA for next round selection were as same as the described above.

2.4. Binding-affinity measurements with BLI assay

The affinities of selected aptamers of HPV L1 were measured by BLI instrument (Octet K2 system, Molecular Devices LLC, San Jose, CA, USA). We loaded the biotinylated L1 protein (or aptamers, 100 nM) on the SA-sensors, followed by flowing the aptamers (or L1 protein, 200 nM) through the aptamer-immobilized sensor, then the sensor was washed with PBST to allow the aptamers (or protein) disassociation. The aptamers with the highest affinity were chosen for the detailed BLI-kinetic analysis by loading aptamers (100 nM) and flowing the protein at various concentrations to determine the average K_d value.

2.5. Molecular docking

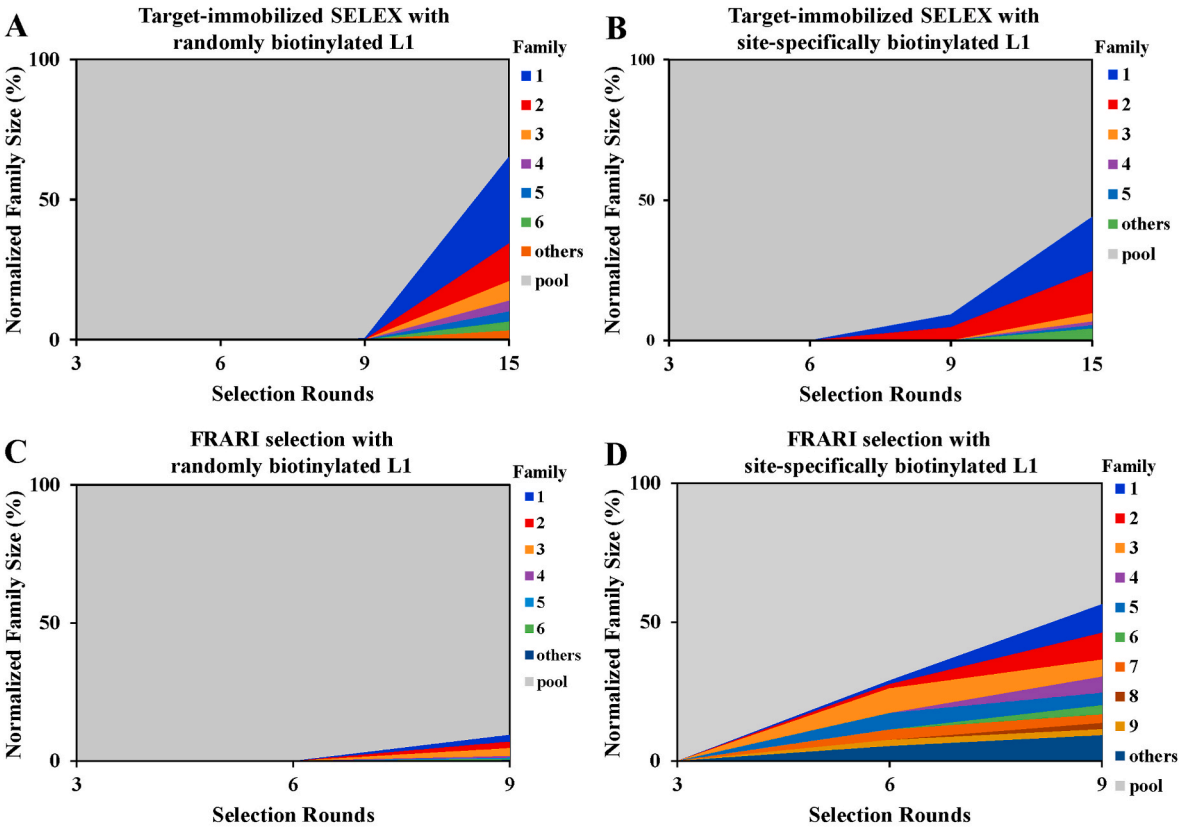
The secondary structures of aptamers were predicted by UNAfold web server (http://www.unafold.org/mfold/applications/dna-folding-form.php) and ImGQfinder web server (http://imgqfinder.niifhm.ru). The tertiary structure of G-quadraplex was predicted by 3D-NuS web server (https://iith.ac.in/3dnus/Quadruplex.html), for example the G-quadraplex of S4-29 aptamer. Other tertiary structures (e.g., R3-30 and R5-36) were predicted with RNAComposer server (https://rnacomposer.cs.put.poznan.pl). As the RNAComposer was developed for RNA structure prediction, we first predicted the RNA structures based on the DNA sequences, and the RNA structures offered approximate DNA foldings, followed by converting RNA to DNA with the Biovia Discovery Studio software. The converted structures were finally optimized by the automated QRNAS software to minimize the energy of base pairs, hydrogen bonds, backbone irregularities and custom restraints [38,39]. The tertiary structure of HPV16 L1 was determined in literature (RCSB PDB ID: 1DZL), followed by the water removal with PyMOL software. Subsequently, the HDOCK web service (http://hdock.phys.hust.edu.cn) was applied for docking simulation [40]. Finally, the interacting residues between HPV16 L1 and the aptamers in docking models were identified by the PLIP web server (https://plip-tool.biotec.tu-dresden.de/plip-web/plip/index).

2.6. Clinical detection of HPV subtypes with aptamers

HPV L1 protein was gradiently diluted with PBST (0.02% Tween 20) or cell lysis buffer to a range of 10^{-1} to 10^4 ng/mL. The MBs immobilized with L1 aptamer R3-30 (50 μg; as aptamer1 in Fig. S13) were added to each L1 protein dilution (50 μL), followed by incubating at room temperature for 1 h to form the aptamer1-L1 complexes and washing twice with PBST to remove non-bound L1. The RCA products (4 μL; containing aptamer2) were added to the complexes, followed by incubating at room temperature for 1 h to form the aptamer1-L1-aptamer2 complexes, and washing twice with PBST to remove the unbound RCA products. The beads were resuspended with 1 × NEB 3.1 buffer (50 μL), followed by addition of the Cas12a-crRNA complex [4 μL; pre-assembled by mixing and incubating Cas12a (400 nM, final concentration) and crRNA (500 nM, final concentration) for 30 min at 37 °C] and FQ-probe (4 μL, 10 μM) for releasing fluorescent signals. The mixture was incubated at 37 °C for 2 h to allow the strong fluorescent signal for the detection and measurement (λ_{ex} = 494 nm; λ_{em} = 522 nm). The measured fluorescent signal was deducted with the background signal (NS, generated in the absence of RCA products), thereby offering the normalized fluorescent intensity (ΔFI) for the quantitative analysis. Further, the limit of detection (LOD) was defined as NS + 3SD, where SD was the standard deviation. The specificity of the FRARI detection was determined by investigating different protein samples (10 μg/mL), including HPV L1, HPV E6, SARS-CoV-2 N protein, SARS-CoV-2 RBD, BSA, HSA and 10% serum.

Though urine samples are desired (as their collections are easy and patient-friendly), urine samples are normally used for the HPV research only, while cervical tissue samples are the most frequent sample types for HPV diagnosis. Therefore, the FRARI detection method has been developed and evaluated with spiked urine and cervical tissue samples. Briefly, urine and cervical tissue lysate samples were spiked with L1 protein on a gradient of 10^{-1} to 10^4 ng/mL followed by the detection with our established method.

For clinical samples, the routine treatments were necessary before detection. For urine samples, urines (1 mL) were centrifuged at 3000 rpm for 5 min to collect the precipitates, which were resuspended in the cell lysis buffer (50 μL), followed by incubating the mixture for 15 min on ice. For cervical tissue samples, cervical swab specimens were



E

FRARI selection with randomly biotinylated L1

	20-mer Arm Sequence		20-mer Arm Sequence
R1	AGCGTCGAATACCACTACAG	CCCGACGATTGCCCCCTGACGCAAGGGTCGTTCGGGAAGC	GACTGGTGCTCGAGGTAATC
R2	********************	GGCCAACCTTTCTGTCTGTGCCCTGAGCCGTCTGAGGGGT	********************
R3	********************	GCTAGCGACTCCGGCAGTACTGTGCGGGGCGGTCGTTTGA	********************
R4	********************	TCGAATAACCGCTGTCCGACGCAGGACTTAGAAGACATGT	********************
R5	********************	GTGTCCCGTCATCCCTAGCTTTGGACTAGCCCGAAGAGGT	********************
R6	********************	AGGCGCCATTAACTCGGGCTACCACCGCTGTCTGACGCAA	********************

FRARI selection with site-specifically biotinylated L1

	20-mer Arm Sequence		20-mer Arm Sequence
S1	AGCGTCGAATACCACTACAG	TCGTATAACCGCTGTCCGACGCAGGACTTAGAAGACATGT	GACTGGTGCTCGAGGTAATC
S2	********************	AGGCGCCATTAACTCGGGCTACCACCGCTGTCTGACGCAA	********************
S3	********************	TTTGCAGTTACAGCTAACGGCGGACTCCGAAATGCCCCCT	********************
S4	********************	CCCATGGGTTCGGCTGGTTGGCATGGGCGGATCTCTACCC	********************
S5	********************	AGGCCGCGCCTGTCGTTCACATGCCTAACGAACAACCCTT	********************
S6	********************	GATAAACAATCAAGTCAACGAAGTATCTCAACTCCGGACC	********************
S7	********************	CCGTCGTTCACCCGATTCTAACCTTTACTACTATTCTGCC	********************
S8	********************	CTATGACTTAGACCAGCCTATAGGACGCTACGCTTGTTGA	********************
S9	********************	CGATCGTCGGCGCTACAACTGTGGCATGCGAATCCATCCC	********************

Fig. 2. Efficiency comparison between conventional and FRARI selections based on SA-MBs. The pools represented the unclustered sequences. (A) Target-immobilized SELEX with randomly-biotinylated L1; (B) Target-immobilized SELEX with site-specifically-biotinylated L1; (C) FRARI selection with randomly biotinylated L1; (D) FRARI selection with site-specifically biotinylated L1. (E) The most abundant aptamer sequences in each family classified on the bases of many sequencies isolated after 9 rounds of the FRARI selections.

washed thoroughly by PBST (1 mL, 0.02% Tween 20), followed by centrifuging the suspensions at 3000 rpm for 5 min to collect the precipitates. Then the precipitates were resuspended in cell lysis buffer (500 μL), followed by incubating for 15 min on ice. These cell lysates were analyzed with our established method. The sample was positive when its ΔFI was larger than LOD, while it was negative when its ΔFI was smaller than LOD.

3. Results and discussion

3.1. FRARI selection based on SA-MB pull-down

We have established a new strategy allowing the free interaction between the biotinylated targets and potential aptamers for aptamer selection, namely FRARI selection, and its principle was shown in Fig. 1. Briefly, a negative selection was performed with SA-MBs or BLI SA-sensors on the initial ssDNA library to remove the non-specific binders and generate the optimized ssDNA library, and the biotinylated targets were incubated with the library in a free mode to form their complexes, followed by the complex pulling-down with the SA-MBs or BLI SA-sensors. After the washing, elution, amplification and single-strand preparation, the obtained sequences were used as the library for the next round of FRARI selection.

The efficient enrichment of target-aptamer complexes is desired for the FRARI selection. As Biotin-Avidin System (BAS) is one of the most specific and stable systems ($K_d = 10^{-14}$ M) in various environments (e.

g., pH and serum) and denaturing reagents (e.g., urea and guanidine hydrochloride) [41], it was chosen to pull-down the aptamer-ligand complexes. To achieve the highly-efficient selection, we used two biotinylation strategies: the random cross-linking (Fig. S1A) and the site-specific modification (Fig. S1B; on the avi tag with BPL [42]). Further, experimentally, we assessed the efficiency of capturing ligands by BAS. We found that using both biotinylation strategies, over 90% capturing efficiency was achieved, when the weight ratio between the protein and the SA-MBs was proximately 1:80; this ratio was determined by varying quantities of proteins or SA-MBs while keeping the other one constant (Figs. S2A–D).

Furthermore, the incubation time between the targets and beads was optimized as well (Fig. S2E). In addition, we found that in complex environments (such as serum), the pull-down with BAS was efficient (Fig. S2F), indicating that our FRARI selection system for aptamers can be applied under challenging conditions. As L1 proteins have the high sequence homology and similar structures, to illustrate our strategy and detect HPV subtypes, we selected effective HPV L1 protein aptamers, thereby demonstrating a new selection strategy with high efficiency.

3.2. Efficiency of FRARI selection

Firstly, we selected HPV L1 aptamers via the traditional target-immobilized SELEX, where the target proteins were immobilized on the surface of the SA-MBs. By applying the two biotinylation strategies (random or site-specific biotinylation), we parallelly performed 15 rounds of selections with stringent treatments, including the bead-negative screening, short incubation time for target-library interaction, and serum adding environmental complexity. To monitor the selection progress, the enriched pools were analyzed after each selection cycle (Figs. S3A–B); R_0 represented the binding of the initial ssDNA library to the SA-MBs. We classified the selected sequences with FASTAptamer software clustering sequences into families [43]. Our results (Fig. 2A–B) indicated that using the site-specific strategy, some L1 aptamers were enriched after 9 rounds of selection (the normalized total family size: 8%; 15-round selection enriched 44%), while using the random one, they were generated after 15 rounds (the total size: 65%), indicating that the former strategy is better than the later one. Using the traditional strategy, we found that 15-round selections were necessary to achieve the significant enrichments, and the target-efficiently-binding aptamers were present in Fig. S4.

To further shorten the selection cycle and enhance the selection efficiency, we explored the FRARI selection by taking advantage of free target interaction with the library, in the selection solution. Using the random biotinylation, the aptamers with significant binding were enriched after 9 rounds of selection (the normalized size of total families: 15%; Fig. 2C), while using the site-specific one, they were generated after just 6 rounds (the size of total families: 29%; Fig. 2D). These selection results indicated that the site-specific biotinylation strategy is better than the random one. The 9-round selection sequences were clustered and analyzed (Figs. S3C–D), and the target-efficiently-binding aptamers were present in Fig. 2E. Our results demonstrated that our FRARI strategy is more efficient than the tradition SELEX.

Our results indicated that the combination of the site-specific biotinylation and free-target strategies offered the efficient aptamers in only 6 rounds of selection, significantly improving the selection

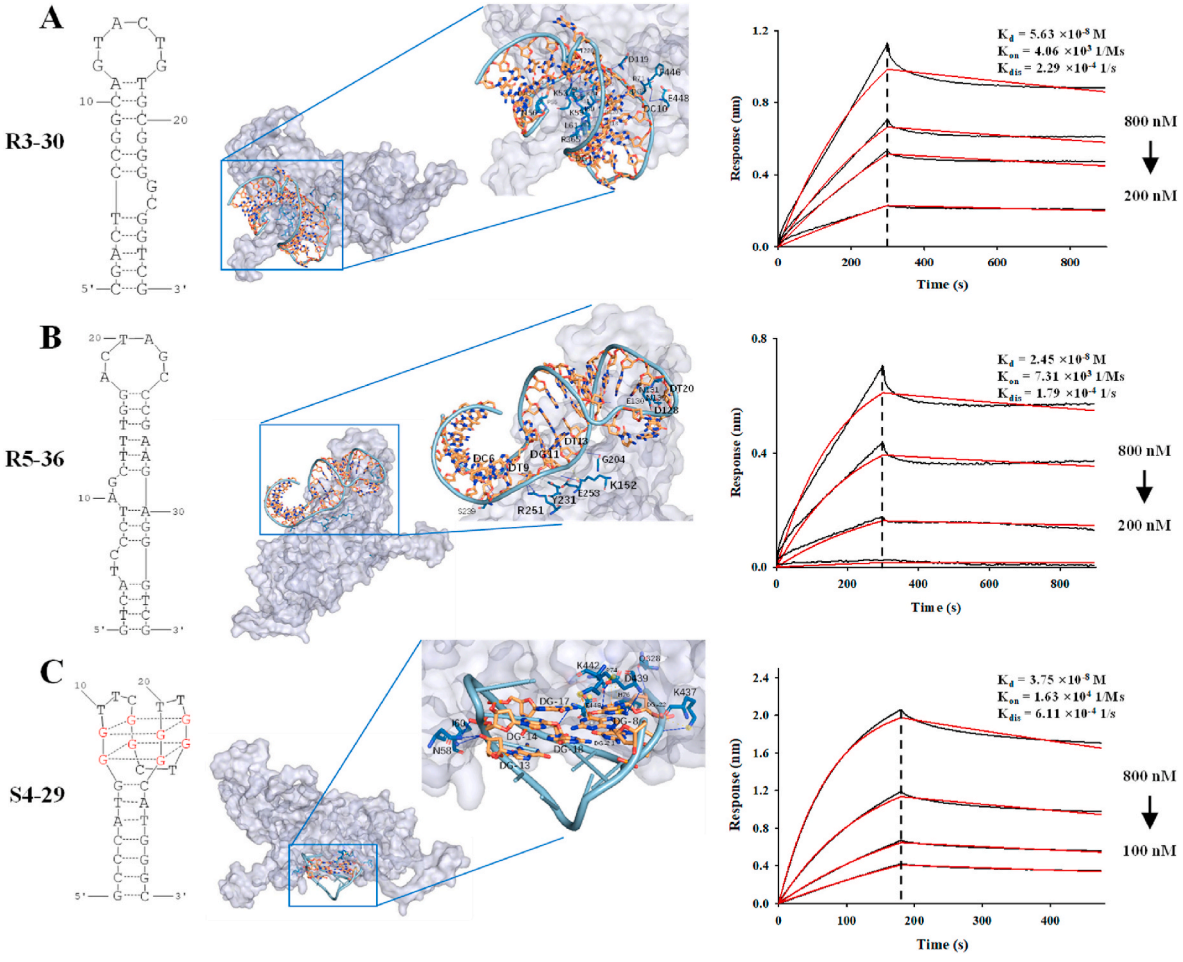


Fig. 3. Secondary structures, docking and affinity analysis of the optimized aptamers from FRARI selection. (A) R3-30 truncated from R3 in Fig. 2; (B) R5-36 truncated from R5; (C) S4-39 truncated from S4.

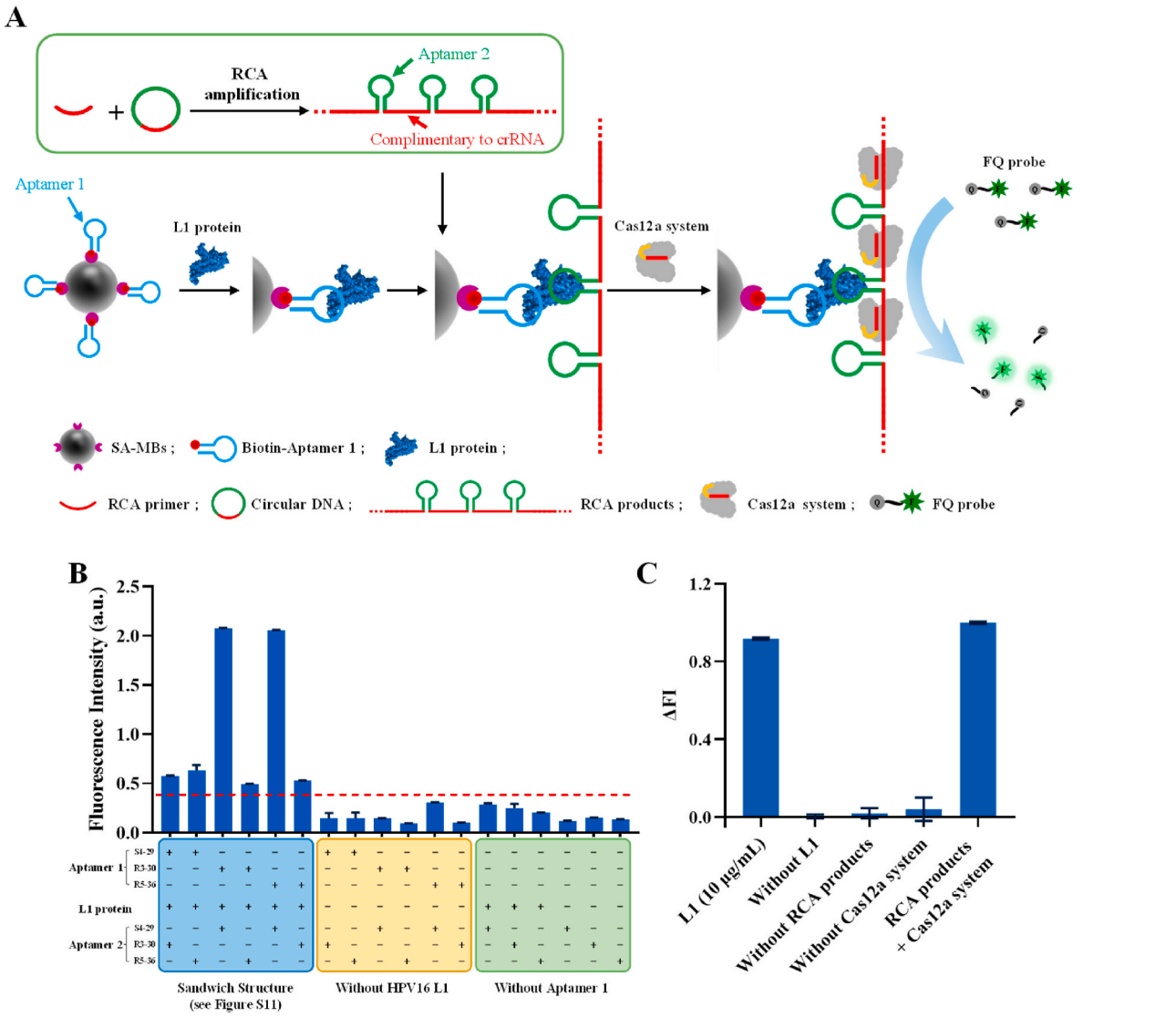


Fig. 4. Detection design of aptamer sandwich. (A) Scheme of the design of sandwich aptasensor assisted with RCA and CRISPR/Cas12a; (B) Optimization of the aptamer combination; (C) Verification of the detection design.

efficiency. The high efficiency can be attributed to the two major reasons. Firstly, to avoid the conformational changes and losses of binding sites caused by the target or library immobilizations on solid surfaces, the free mode of target-aptamer interaction provided the structural integrity of the targets and the ssDNA library for their convenient binding. The non-specific interactions caused by the inappropriate immobilizations were no longer hindrances for selecting aptamers efficiently. Secondly, to avoid the random modification influence on protein conformations, causing the interaction verification between the targets and aptamers in each selection cycle, the site-specific biotinylation strategy was explored and found to be more efficient than the random one.

In addition, we explored the FRARI selection under the challenging conditions, such as complex environmental interference (by adding serum, which can help obtaining stable aptamers that tolerate diverse application environments). We found that our FRARI strategy was tolerant of challenging conditions and allowed efficient selection of aptamers, such as the L1 aptamers.

3.3. FRARI selection based on BLI binding

To further explore the ability of the FRARI strategy to be used on different sensors, by taking advantage of the BLI sensor (for highly-sensitive dynamic binding), we directly explored the FRARI selection. The sensor immobilized with SA was used to capture the biotinylated target-aptamer complexes, where two biotinylation strategies (random or site-specific biotinylation) were investigated. Using both strategies, when the BLI signal is not saturated (Figs. S5A–C, i.e., the amount of randomly-biotinylated L1 and site-specifically-biotinylated L1 was less than 0.625 g and 0.3 g, respectively), the capture efficiency could reach up to 90%. And we performed 9 rounds of the aptamer selection (Figs. S6A–B), followed by sequencing and FASTAptamer clustering (Fig. S7). We found that the random strategy required 9 rounds to offer the aptamer clustering (Fig. S7A), while the site-specific strategy only needed 6 rounds (Fig. S7B). After 9 rounds of selection, the site-specific strategy allowed the 50% clustering of total family size. Notably, Family 1 from the site-specific strategy dominated 43% of the family size (Fig. S7B), where the most abundant sequence was consistent with S4 in MB-based FRARI strategy. The results indicated that the FRARI selection was also applicable to the BLI sensor, and many low-affinity families were excluded by the selection, which could be attributed to the fact that BLI sensor has a smaller specific surface area and less non-specific binding. Similarly, as well as the MB-based FRARI strategy, the BLI-based method with the site-specific biotinylation offers high efficiency

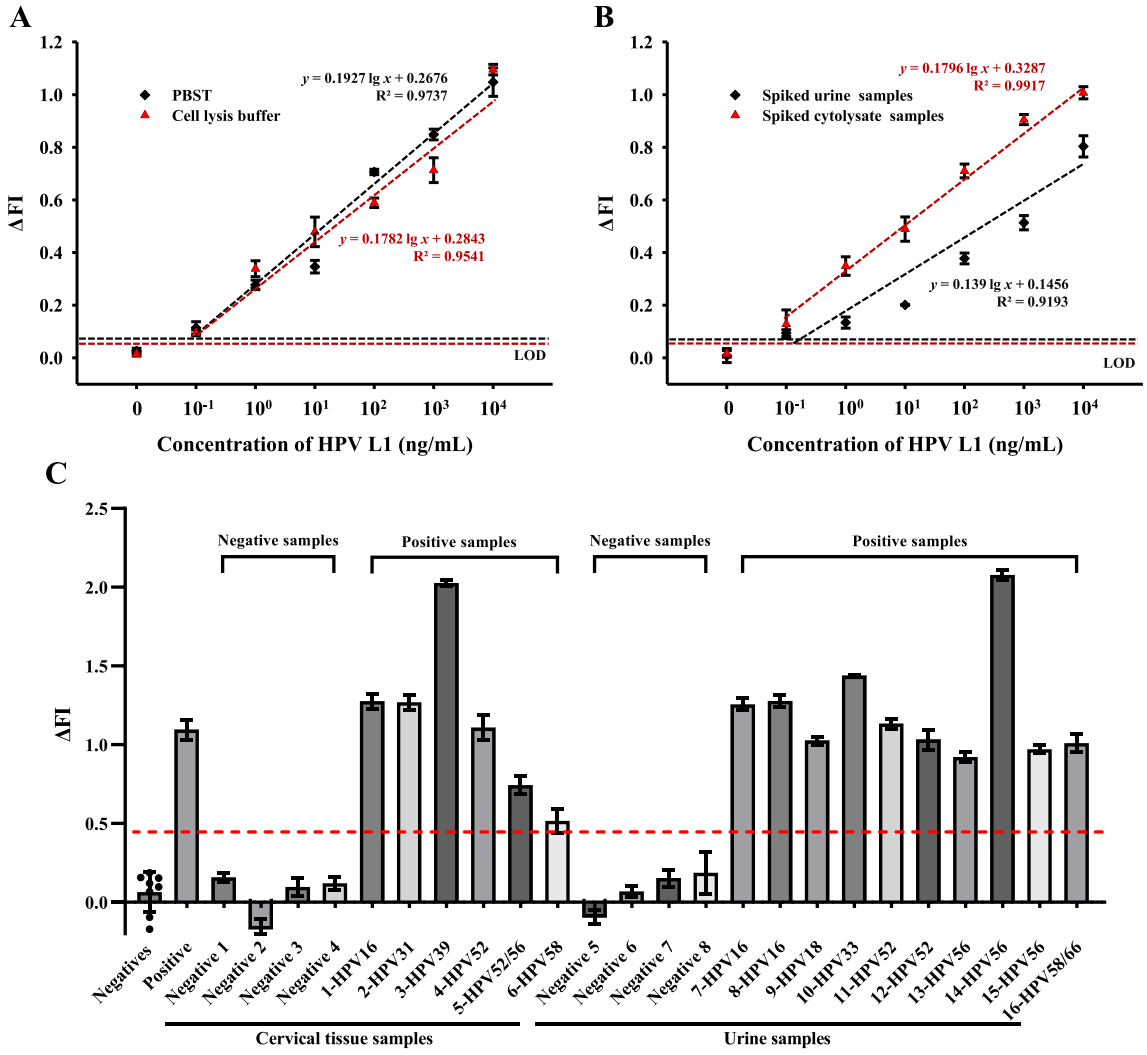


Fig. 5. Detection of clinical HPV samples. (A) The working curves in PBST and cell lysis buffers. (B) The working curves in clinical urine sample and cervical-tissue-lysate sample spiked with L1 protein. (C) Clinical detection of many HPV subtypes confirmed by the conventional method (see the method section).

for aptamer selection. Further, the MB-based strategy doesn't rely on expensive instruments and is easy to operate, making it more convenient for universal applicability.

3.4. Affinity studies on HPV L1 aptamers

The selected sequences of L1 aptamers, clustered for a total of 16 families (Table S2), were used for affinity analysis (Figs. S8 and S9). Among them, R3, R5 and S4 aptamers offered high affinities (25.9 × , 7.33 × and 4.93 × 10^{-8} M, respectively; Fig. S10). By generating the secondary structures of these aptamers with NUPACK (http://www.nupack.org; Fig. S10), we analyzed and truncated the original aptamer sequences, and obtained the shorter sequences (Table S3), including R3-30 (30 nt), R5-36 (36 nt) and S4-29 (29 nt). After analyzing them with UNAFold and ImGQfinder softwares, we found that R5-36 formed a stem-loop structure, while the structures of S4-29 and R3-30 were predicted to be a G-quadraplex or stem-loop structure. To test whether they contained G-quadruplex structures, we designed the G-quadraplex confirmation experiments, such as the thioflavin (THT) fluorescence and Circular dichroism (CD) analysis. In our experiments, we found that S4-29 formed a G-quadruplex, while R3-30 didn't (Figs. S11A–B). CD analysis further confirmed S4-29 forming an antiparallel G-quadruplex, as it generated the CD signals at approximately 260 and 290 nm (Fig. S11C) [44], while R3-30 didn't but probably formed a stem-loop structure. Further, we proposed the secondary structures of these three aptamers, followed by molecular docking between L1 protein and the aptamer 3D structures simulated with RNAComposer and Biovia Discovery Studio softwares (Fig. 3), implying the three aptamers binding to L1 protein at different sites. Furthermore, we performed the affinity measurements of these aptamers with BLI, and found that the K_d values of R3-30, R5-36 and S4-29 were 5.63 × , 2.45 × and 3.75 × 10^{-8} M, respectively (Fig. 3), indicating that the FRARI selection can offer aptamers with high affinity. Moreover, we performed the specificity measurements of these aptamers with BLI and different non-specific proteins (BSA, HSA and E6 proteins), and we found that these aptamers only interacted with L1 protein, but didn't with other proteins, indicating the high specificity of these aptamers (Fig. S12).

3.5. Designing aptamer-detection sandwich

We developed a rapid HPV detection method (FRARI detection assay; Fig. 4A), by immobilizing the biotinylated L1 aptamers on SA-MBs, followed by capturing L1 protein in the samples. Further, the captured protein was used as the target for the binding of the second aptamer, which was rolling-circle amplified (RCA) [45] and separated by a spacer. Furthermore, the spacer was recognized and bound by Cas12a-crRNA

[46,47] for cleaving the substrates, generating the fluorescent signal for the detection.

In the aptamer-based target detection, a stable and specific sandwich structure is critical. In order to identify the aptamers for the sandwich construction, firstly, we evaluated the aptamers for the aptamer1-target-aptamer2 structure (Fig. S13). We found that the combination of R3-30 or R5-36 (as aptamer1) and S4-29 (as aptamer2) was most successful (Fig. 4B), thereby offering R3-30 and S4-29 as aptamer1 and 2 for the sandwich structure, respectively. Finally, the sandwich design and the FRARI detection were confirmed experimentally by positive and negative tests (Fig. 4C).

3.6. Clinical detection of HPV subtypes with aptamers

Based on the established FRARI detection method, the sensitivity for HPV L1 detection was explored. We found that the limit of detection (LOD) in PBST and cell-lysis buffer were similar (LOD: 0.1 ng/mL; Fig. 5A). Further, we explored the specificity of the FRARI detection in the presence of various interferants, including HPV E6, SARS-Covid-2 N protein, SARS-Covid-2 RBD, BSA, HSA and 10% serum. We found that the FRARI detection was specific, as these interferants didn't generate significant signals (Fig. S14). Furthermore, to study the applicability of FRARI detection with clinical samples, the samples of urines and cervical tissue lysates spiked with L1 protein were studied. We found that the LODs for the urine and lysate samples were similar (LOD: 0.1 ng/mL; Fig. 5B) to the LOD in just buffers, indicating that the complex environments didn't significantly disrupt our FRARI detection. Finally, we investigated our FRARI detection method with the clinically-negative or -positive HPV samples confirmed with the standard strategy [48]. In details, 10 cervical tissue samples (including 4 negative ones and 6 positive ones) and 14 urine samples (including 4 negative ones and 10 positive ones) were analyzed with our strategy. As the L1 proteins from HPV subtypes have the high sequence homology (Fig. S15) and similar structures, our results have shown that the FRARI detection strategy was able to detect several HPV subtypes in clinical samples (Fig. 5C), including urine and cervical tissue samples. Particularly, the ability to detect HPV in urine samples was of great value for developing convenient HPV detection methods, due to the ease and friendliness of the sample collection. Our results demonstrated that the FRARI detection was sensitive, accurate and robust for L1 protein detection, suggesting that the aptamers selected with our FRARI strategies could tolerate the complex samples and environments.

4. Conclusion

In summary, we have established the FRARI selection method on the SA-MBs and BLI sensors by combining the free target and site-specific biotinylation strategies, which is highly-efficient and convenient. By using our new strategy, clinically-useful aptamers can be isolated in the complex environments (such as serum) and under strict conditions. Further, with our new strategy, we have successfully selected the HPV L1 aptamers for simultaneously detecting various HPV subtypes, thereby offering a convenient method for HPV screening. Furthermore, various HPV subtypes in clinical samples (such as urines collected easily and patient-friendly) have been detected, indicating the effectiveness and practicability of FRARI in selecting aptamers for clinical applications.

Credit author statement

Zhen Huang conceived and directed the project. Guotai Yang and Zhen Huang designed the research. Guotai Yang performed most of the experiments. Wei Li and Shun Zhang helped express and purify proteins. Wei Li helped perform the target-immobilized SELEX assay and BLI experiments. Shun Zhang and Bei Hu analyzed the data. Guotai Yang and Zhen Huang wrote the manuscript.

Declaration of competing interest

The authors declare that they have no known competing financial interests or personal relationships that could have appeared to influence the work reported in this paper.

Data availability

Data will be made available on request.

Acknowledgements

This work was supported by the Sichuan Province Science and Technology Support program (2022YFSY0013, 2023NSFSC1107 and 2021YJ0319), the Open Research Fund of State Key Laboratory of Southwestern Chinese Medicine Resources (SKLTCM202202), the National Key Research and Development Program of China (2022YFC2303700), the Natural Science Foundation - Youth Science Foundation Project (22107079), and the China Postdoctoral Science Foundation (2020M673205).

Appendix A. Supplementary data

Supplementary data to this article can be found online at https://doi.org/10.1016/j.talanta.2023.125039.

References

[1] A.D. Ellington, J.W. Szostak, *In vitro* selection of RNA molecules that bind specific ligands, Nature 346 (6287) (1990) 818–822, https://doi.org/10.1038/346818a0.
[2] C. Tuerk, L. Gold, Systematic evolution of ligands by exponential enrichment: RNA ligands to bacteriophage T4 DNA polymerase, Science 249 (4968) (1990) 505–510, https://doi.org/10.1126/science.2200121.
[3] D.E. Huizenga, J.W. Szostak, A DNA aptamer that binds adenosine and ATP, Biochemistry 34 (2) (1995) 656–665, https://doi.org/10.1021/bi00002a033.
[4] S.M. Nimjee, R.R. White, R.C. Becker, B.A. Sullenger, Aptamers as therapeutics, Annu. Rev. Pharmacol. Toxicol. 57 (2017) 61–79, https://doi.org/10.1146/annurev-pharmtox-010716-104558.
[5] K.S. Park, Nucleic acid aptamer-based methods for diagnosis of infections, Biosens. Bioelectron. 102 (2018) 179–188, https://doi.org/10.1016/j.bios.2017.11.028.
[6] P. Tran, D. Xiang, T. Tran, W. Yin, W. Duan, Exosomes and nanoengineering: a match made for precision therapeutics, Adv. Mater. 32 (18) (2019), 1904040, https://doi.org/10.1002/adma.201904040.
[7] X. Li, K. Feng, L. Li, L. Yang, X. Pan, Y.H. Safari, C. Cui, J. Li, M. Leonid, Y. Sun, Lipid-oligonucleotide conjugates for bioapplications, Natl. Sci. Rev. 7 (12) (2020) 1933–1953, https://doi.org/10.1093/nsr/nwaa161.
[8] N. Duan, C. Li, X. Zhu, S. Qi, Z. Wang, S. Wu, Simultaneous coupled with separate SELEX for heterocyclic biogenic amine-specific aptamers screening and their application in establishment of an effective aptasensor, Sens. Actuators B Chem. Pt. 1 (2022) 352, https://doi.org/10.1016/j.snb.2021.130985.
[9] W. Guo, C. Zhang, T. Ma, X. Liu, Z. Chen, S. Li, Y. Deng, Advances in aptamer screening and aptasensors' detection of heavy metal ions, J. Nanobiotechnol. 19 (1) (2021) 166, https://doi.org/10.1186/s12951-021-00914-4.
[10] P.R. Gruenke, R. Aneja, S. Welbourn, O.B. Ukah, S.G. Sarafianos, D.H. Burke, M. J. Lange, Selection and identification of an RNA aptamer that specifically binds the HIV-1 capsid lattice and inhibits viral replication, Nucleic Acids Res. 50 (3) (2022) 1701–1717, https://doi.org/10.1093/nar/gkab1293.
[11] E. Duchardt-Ferner, M. Juen, B. Bourgeois, T. Madl, C. Kreutz, O. Ohlenschläger, J. Wöhnert, Structure of an RNA aptamer in complex with the fluorophore tetramethylrhodamine, Nucleic Acids Res. 48 (2) (2020) 949–961, https://doi.org/10.1093/nar/gkz1113.
[12] L. Civit, S.M. Taghdisi, A. Jonczyk, S. Haßel, C. Gröber, M. Blank, H.J. Stunden, M. Beyer, J. Schultze, E. Latz, Systematic evaluation of cell-SELEX enriched aptamers binding to breast cancer cells, Biochimie 145 (2018) 53–62, https://doi.org/10.1016/j.biochi.2017.10.007.
[13] Z. Huang, J.W. Szostak, Evolution of aptamers with a new specificity and new secondary structures from an ATP aptamer, RNA 9 (12) (2003) 1456–1463, https://doi.org/10.1261/rna.5990203.
[14] L. Zhou, P. Li, M. Yang, Y. Yu, Y. Huang, J. Wei, S. Wei, Q. Qin, Generation and characterization of novel DNA aptamers against coat protein of grouper nervous necrosis virus (GNNV) with antiviral activities and delivery potential in grouper cells, Antivir. Res. 129 (2016) 104–114, https://doi.org/10.1016/j.antiviral.2016.02.009.
[15] Y. Mao, J. Gu, D. Chang, L. Wang, L. Zheng, Evolution of a highly functional circular DNA aptamer in serum, Nucleic Acids Res. 48 (19) (2020) 10680–10690, https://doi.org/10.1093/nar/gkaa800.

[16] Y. Han, D. Diao, Z. Lu, X. Li, Q. Guo, Y. Huo, Q. Xu, Y. Li, S. Cao, J. Wang, Selection of group-specific phthalic acid esters binding DNA aptamers via rationally designed target immobilization and applications for ultrasensitive and highly selective detection of phthalic acid esters, Anal. Chem. 89 (10) (2017) 5270–5277, https://doi.org/10.1021/acs.analchem.6b04808.
[17] M. Cho, S. Soo Oh, J. Nie, R. Stewart, M. Eisenstein, J. Chambers, J.D. Marth, F. Walker, J.A. Thomson, H.T. Soh, Quantitative selection and parallel characterization of aptamers, Proc. Natl. Acad. Sci. U. S. A. 110 (46) (2013) 18460–18465, https://doi.org/10.1073/pnas.1315866110.
[18] M.A. Vorobyeva, A.S. Davydova, P.E. Vorobjev, A.G. Venyaminova, Key aspects of nucleic acid library design for *in vitro* selection, Int. J. Mol. Sci. 19 (2) (2018) 470, https://doi.org/10.3390/ijms19020470.
[19] S.D. Mendonsa, M.T. Bowser, *In vitro* evolution of functional DNA using capillary electrophoresis, J. Am. Chem. Soc. 126 (1) (2004) 20–21, https://doi.org/10.1021/ja037832s.
[20] G. Yang, Z. Li, I. Mohammed, L. Zhao, W. Wei, H. Xiao, W. Guo, Y. Zhao, F. Qu, Y. Huang, Identification of SARS-CoV-2-against aptamer with high neutralization activity by blocking the RBD domain of spike protein 1, Signal Transduct. Targeted Ther. 6 (1) (2021) 227, https://doi.org/10.1038/s41392-021-00649-6.
[21] Q. Zhou, X. Xia, Z. Luo, H. Liang, E. Shakhnovich, Searching the sequence space for potent aptamers using SELEX in silico, J. Chem. Theor. Comput. 11 (12) (2015) 5939–5946, https://doi.org/10.1021/acs.jctc.5b00707.
[22] N. Qiao, J. Li, X. Wu, D. Diao, X. Lou, Speeding up *in vitro* discovery of structure-switching aptamers via magnetic cross-linking precipitation, Anal. Chem. 91 (21) (2019) 13383–13389, https://doi.org/10.1021/acs.analchem.9b00081.
[23] M. Berezovski, A. Drabovich, S.M. Krylova, M. Musheev, V. Okhonin, A. Petrov, S. N. Krylov, Nonequilibrium capillary electrophoresis of equilibrium mixtures: a universal tool for development of aptamers, J. Am. Chem. Soc. 127 (9) (2005) 3165–3171, https://doi.org/10.1021/ja042394q.
[24] A.M. Yoshikawa, A. Rangel, T. Feagin, E.M. Chun, L. Wan, A. Li, L. Moeckl, D. Wu, M. Eisenstein, S. Pitteri, H.T. Soh, Discovery of indole-modified aptamers for highly specific recognition of protein glycoforms, Nat. Commun. 12 (1) (2021) 7106, https://doi.org/10.1038/s41467-021-26933-1.
[25] S.S. Oh, K. Plakos, X. Lou, Y. Xiao, Soh, *In vitro* selection of structure-switching, self-reporting aptamers, Proc. Natl. Acad. Sci. U. S. A. 107 (32) (2010) 14053–14058, https://doi.org/10.1073/pnas.1009172107.
[26] B. Jonathan, A. Patrick, D.M. Brown, G. Louis, T. Craig, G. Larry, RNA ligands to human nerve growth factor, Nucleic Acids Res. 23 (16) (1995) 3198–3205, https://doi.org/10.1093/nar/23.16.3198.
[27] Y.Z. Wei, W. Zhang, Z. Liu, L. Cong, C.J. Yang, Highly parallel single-molecule amplification approach based on agarose droplet polymerase chain reaction for efficient and cost-effective aptamer selection, Anal. Chem. 84 (1) (2012) 350–355, https://doi.org/10.1021/ac2026942.
[28] E. Dausse, A. Barré, A. Aimé, A. Groppi, A. Rico, C. Ainali, G. Salgado, W. Palau, E. Daguerre, M. Nikolski, J.J. Toulmé, C. Di Primo, Aptamer selection by direct microfluidic recovery and surface plasmon resonance evaluation, Biosens. Bioelectron. 80 (2016) 418–425, https://doi.org/10.1016/j.bios.2016.02.003.
[29] M. Mukherjee, P. Appaiah, S. Sistla, B. Bk, P. Bhatt, bio-layer interferometry-based SELEX and label-free detection of patulin using generated aptamer, J. Agric. Food Chem. 70 (20) (2022) 6239–6246, https://doi.org/10.1021/acs.jafc.2c01591.
[30] J. Wang, Q. Gong, N. Maheshwari, M. Eisenstein, M.L. Arcila, K.S. Kosik, H.T. Soh, Particle display: a quantitative screening method for generating high-affinity aptamers, Angew Chem. Int. Ed. Engl. 53 (19) (2014) 4796–4801, https://doi.org/10.1002/anie.201309334.
[31] A. Ozer, B.S. White, J.T. Lis, D. Shalloway, Density-dependent cooperative non-specific binding in solid-phase SELEX affinity selection, Nucleic Acids Res. 41 (14) (2013) 7167–7175, https://doi.org/10.1093/nar/gkt477.
[32] R.K. Mosing, S.D. Mendonsa, M.T. Bowser, Capillary electrophoresis-SELEX selection of aptamers with affinity for HIV-1 reverse transcriptase, Anal. Chem. 77 (19) (2005) 6107–6112, https://doi.org/10.1021/ac050836q.
[33] Q. Kong, F. Yue, M. Liu, J. Huang, F. Yang, J. Liu, J. Li, F. Li, X. Sun, Y. Guo, Y. Zhu, Non-immobilized GO-SELEX of aptamers for label-free detection of thiamethoxam in vegetables, Anal. Chim. Acta 1202 (2022), 339677, https://doi.org/10.1016/j.aca.2022.339677.
[34] Y. Yue, D. Zhang, K. Tian, D. Ni, F. Guo, Z. Yu, P. Wang, P. Liang, Screening and evaluation of thiamethoxam aptamer based on pressurized GO-SELEX and its sensor application, Biosensors 13 (2) (2023) 155, https://doi.org/10.3390/bios13020155.
[35] X. Zhang, G. Yang, W. Liu, Q. Liu, Z. Wang, K. Fan, F. Qu, Y. Huang, Screening and identification of ssDNA aptamers for low-density lipoprotein (LDL) receptor-related protein 6, Molecules 28 (9) (2023) 3838, https://doi.org/10.3390/molecules28093838.
[36] K. Adamiak, A. Sionkowska, Current methods of collagen cross-linking: review, Int. J. Biol. Macromol. 161 (2020) 550–560, https://doi.org/10.1016/j.ijbiomac.2020.06.075.
[37] Y. Li, S. Rui, Expression and purification of *E. coli* BirA biotin ligase for in vitro biotinylation, Protein Expr. Purif. 82 (1) (2012) 162–167, https://doi.org/10.1016/j.pep.2011.12.008.
[38] R. Oliveira, E. Pinho, A.L. Sousa, Ó. Dias, N.F. Azevedo, C. Almeida, Modelling aptamers with nucleic acid mimics (NAM): from sequence to three-dimensional docking, PLoS One 17 (3) (2022), e0264701, https://doi.org/10.1371/journal.pone.0264701.
[39] J. Stasiewicz, S. Mukherjee, C. Nithin, J.M. Bujnicki, QRNAS: software tool for refinement of nucleic acid structures, BMC Struct. Biol. 19 (1) (2019) 5, https://doi.org/10.1186/s12900-019-0103-1.
[40] Y. Yan, D. Zhang, P. Zhou, B. Li, S.Y. Huang, HDOCK: a web server for protein-protein and protein-DNA/RNA docking based on a hybrid strategy, Nucleic Acids Res. 45 (W1) (2017) W365–w373, https://doi.org/10.1093/nar/gkx407.
[41] N.M. Green, AVIDIN. 1. The use of (14-c)biotin for kinetic studies and for assay, Biochem. J. 89 (3) (1963) 585–591, https://doi.org/10.1042/bj0890585.
[42] S. Driegen, R. Ferreira, A.V. Zon, J. Strouboulis, M. Jaegle, F. Grosveld, S. Philipsen, D. Meijer, A generic tool for biotinylation of tagged proteins in transgenic mice, Transgenic Res. 14 (4) (2005) 477–482, https://doi.org/10.1007/s11248-005-7220-2.
[43] K.K. Alam, J.L. Chang, D.H. Burke, FASTAptamer: a bioinformatic toolkit for high-throughput sequence analysis of combinatorial selections, Mol. Ther. Nucleic Acids 4 (3) (2015), e230, https://doi.org/10.1038/mtna.2015.4.
[44] C. Okamoto, A. Momotake, Y. Yamamoto, Structural and functional characterization of complexes between heme and dimeric parallel G-quadruplex DNAs, J. Inorg. Biochem. 216 (2021), 111336, https://doi.org/10.1016/j.jinorgbio.2020.111336.
[45] Y. Lv, R. Hu, G. Zhu, X. Zhang, L. Mei, Q. Liu, L. Qiu, C. Wu, W. Tan, Preparation and biomedical applications of programmable and multifunctional DNA nanoflowers, Nat. Protoc. 10 (10) (2015) 1508–1524, https://doi.org/10.1038/nprot.2015.078.
[46] J.S. Chen, E. Ma, L.B. Harrington, M. Da Costa, X. Tian, J.M. Palefsky, J.A. Doudna, CRISPR-Cas12a target binding unleashes indiscriminate single-stranded DNase activity, Science 360 (6387) (2018) 436–439, https://doi.org/10.1126/science.aar6245.
[47] S. Xing, Z. Lu, Q. Huang, H. Li, Y. Wang, Y. Lai, Y. He, M. Deng, W. Liu, An ultrasensitive hybridization chain reaction-amplified CRISPR-Cas12a aptasensor for extracellular vesicle surface protein quantification, Theranostics 10 (22) (2020) 10262–10273, https://doi.org/10.7150/thno.49047.
[48] T. Li, Y. Lai, J. Yuan, The diagnostic accuracy of TCT + HPV-DNA for cervical cancer: systematic review and meta-analysis, Ann. Transl. Med. 10 (14) (2022) 761, https://doi.org/10.21037/atm-22-1732.